Influence of the Inequality Aversion Parameter on the Performance of the Atkinson Index Detector

Dayan A. Guimarães and Luiz G. B. Guedes

***Abstract*— The Atkinson index detector (AID) was recently developed for cooperative spectrum sensing. It is parameterized by the inequality aversion parameter ϵ, which controls sensitivity to data disparities. However, the original publication where the AID was devised did not explore in detail the influence of ϵ in the spectrum sensing performance. This paper addresses this gap by making an in-depth analysis of ϵ in the performance of the AID. It is demonstrated that $\epsilon = 0.1$ yields better performances in the majority of practical scenarios, while $\epsilon = 0.5$ is the best choice for low-complexity computation of the AID test statistic and better performances over Rayleigh fading channels.**

***Keywords*— Atkinson index detector, cognitive radio, dynamic spectrum access, spectrum sensing.**

I. INTRODUCTION

The proliferation of wireless communication systems in recent years has led to a scarcity of available radio-frequency (RF) spectrum. This scarcity is largely attributed to the implementation of fixed spectrum allocation policies, in which a network of primary users (PUs) holds exclusive rights to operate over specific RF bands. However, recent studies have shown that numerous allocated RF bands remain underutilized across different regions and time periods, resulting in inefficient spectrum usage [1].

The RF spectrum scarcity is expected to worsen with the continued expansion of the Internet of Things (IoT), the deployment of 5G networks, and the anticipated development of 6G networks. These technological advancements will demand wider bandwidths, thereby increasing the competition for an already limited spectral resource [1].

One potential approach to improve spectrum utilization involves the implementation of cognitive radio (CR) networks. These networks are capable of identifying unoccupied bands that arise due to the spatiotemporal variability in primary network channel usage [2]. In such scenario, a dynamic spectrum access (DSA) policy can be adopted, enabling secondary users (SUs) with cognitive capabilities to opportunistically access idle frequency bands. The strategy adopted is known as spectrum sensing, which relies on techniques that may or may not incorporate spectrum occupancy databases to identify spectral gaps [1], [3].

Dayan A. Guimarães and Luiz G. B. Guedes are with the National Institute of Telecommunications (Inatel), Santa Rita do Sapucaí, MG, Brazil, e-mail: dayan@inatel.br; luizgustavo.barros@inatel.br. This work was funded by resources from the following agencies: RNP/MCTI (Grant 01245.010604/2020-14), EMBRAPII/MCTI (Grants 052/2023 PPI IoT/Manufatura 4.0, PPE-00124-23), FAPESP (Grants 22/09319-9, 20/05127-2), FAPEMIG (Grants APQ-04523-23, APQ-05305-23, APQ-01558-24, RED-00194-23), and CNPq (Grant 302589/2021-0).

While spectrum sensing performed individually by each SU is susceptible to impairments such as multipath fading, signal shadowing, and the hidden terminal problem, cooperative spectrum sensing (CSS) mitigates these effects by leveraging multiple SUs, thereby improving the accuracy of decisions regarding spectrum occupancy.

This work considers a CSS scheme with distributed detection and centralized decision-making through data fusion. In this configuration, primary signal samples received by the SUs are transmitted to a fusion center (FC), where they are used to compute a test statistic. This statistic is then compared to a decision threshold to generate a global decision on the occupancy state of the monitored frequency band.

A wide range of detection techniques have been proposed for spectrum sensing, from conventional energy detection methods to more recent approaches based on neural networks, machine learning, and artificial intelligence. Other strategies include detectors that exploit cyclostationary features of the signal or eigenvalue-based criteria [3].

More recently, the use of inequality indices has been proposed as an innovative and promising framework for detector design [4]–[9]. These indices, commonly employed in economics and social sciences to quantify income or wealth disparity among individuals or populations, offer a novel perspective in the signal detection area.

The Atkinson index detector (AID) is another inequality index detector that has been recently introduced [10]. It adapted the Atkinson coefficient formula to operate on the elements of the sample covariance matrix (SCM) of the received signal. The resulting AID features low computational complexity, robustness to variations in signal and noise power levels, and the desirable property of constant false alarm rate (CFAR), yet outperforming several conventional detectors in many practical scenarios.

The test statistic of the AID is parameterized by an inequality aversion parameter, ϵ. As the name suggests, the parameter controls the sensitivity of the test statistic to disparities in the input data, i.e. the SCM elements. In [10], only a minor investigation has been made in regard to the influence of ϵ on the performance of the AID. Hence, motivated by the need for more information regarding the choice of this parameter, this paper makes a deep analysis of the influence of ϵ on the performance of the AID, as well as on possible numerical problems that may arise depending on the chosen value of ϵ.

The remainder of this paper is structured as follows: Section II introduces the signal, noise, and channel models. Section III provides a brief overview of the AID, with focus on its inequality aversion parameter. Section IV presents the numerical results and discussions, while Section V concludes the paper.

II. System model

The model adopted herein for CSS with data fusion is the same as the one in [10], ensuring consistency of results and conclusions. Some details are therefore omitted for conciseness, and the reader is referred to [11] for further information.

Spectrum sensing is performed by m SUs uniformly distributed on a circular area of radius r centered at $(0,0)$. Unless stated otherwise, the PU transmitter is positioned at $(x,y)=(r,r)$. Placing the PU transmitter outside the coverage area of the secondary network is a common approach for establishing an exclusion zone, which is a designated region around the PU where SUs are restricted from accessing the spectrum, in order to protect the PU from harmful interference.

Each SU collects n samples of the primary signal during a sensing interval. The samples gathered by all SUs are then transmitted to the FC through error-free control channels, forming the sample matrix $\mathbf{Y}\in\mathbb{C}^{m\times n}$, given by

$$\mathbf{Y}=\mathbf{h}\mathbf{x}^{\mathrm{T}}+\mathbf{V}, \tag{1}$$

where the vector $\mathbf{x}\in\mathbb{C}^{n\times 1}$ contains the primary signal samples, modeled as zero-mean complex Gaussian random variables. The channel vector $\mathbf{h}\in\mathbb{C}^{m\times 1}$ comprises elements h_i, representing the channel gains between the PU transmitter and the ith SU, for $i=1,\dots,m$. The temporal variation of these gains reflects the fading effects due to multipath propagation and SU mobility. Specifically, $\mathbf{h}=\mathbf{G}\mathbf{a}$, where $\mathbf{G}$ is a gain matrix defined later, and $\mathbf{a}\in\mathbb{C}^{m\times 1}$ is a vector of complex Gaussian random variables $a_i\sim\mathcal{CN}[\sqrt{K/(2K+2)},1/(K+1)]$. Here, $K=10^{K^{(\mathrm{dB})}/10}$ denotes the Rice factor of the channels between the PU transmitter and the SUs, with $K^{(\mathrm{dB})}=10\log_{10}(K)$ representing its value in decibels.

Based on the findings reported in [12], the Rice factor $K^{(\mathrm{dB})}$ can be modeled as a Gaussian random variable with mean μ_K and standard deviation σ_K, both expressed in decibels. Typical values of μ_K and σ_K depend on the propagation characteristics of the environment. For example, in urban areas, $\mu_K=1.88$ dB and $\sigma_K=4.13$ dB; in rural or open areas, $\mu_K=2.63$ dB and $\sigma_K=3.82$ dB; and in suburban regions, $\mu_K=2.41$ dB and $\sigma_K=3.84$ dB [12].

The received signal power at the SUs may vary in intensity and over time due to differences in the distances between the PU transmitter and the SUs, as well as due to mobility-induced changes in those distances across different sensing events.

In this context, the previously mentioned gain matrix $\mathbf{G}\in\mathbb{R}^{m\times m}$ is given by $\mathbf{G}=\mathrm{diag}(\sqrt{\mathbf{p}/P_{\mathrm{tx}}})$, where $\mathbf{p}=[P_{\mathrm{rx}1},\dots,P_{\mathrm{rx}m}]^{\mathrm{T}}$ is the vector of PU signal powers received by the m SUs, and $[\cdot]^{\mathrm{T}}$ denotes transposition. Here, P_{tx} represents the PU transmission power in watts, and $\mathrm{diag}(\cdot)$ denotes a diagonal matrix with its main diagonal formed by the vector elements in the argument.

The log-distance path loss model [13] is employed to compute the received signal power at the ith SU, in watts, as

$$P_{\mathrm{rx}i}=P_{\mathrm{tx}}\left(\frac{d_0}{d_i}\right)^{\eta}, \tag{2}$$

where d_0 is a reference distance within the far-field region of the transmitting antenna, d_i is the distance between the PU transmitter and the ith SU, and η is the environment-dependent path loss exponent. All distances are specified in meters.

Discrepancies and fluctuations in the noise power at the SU receivers may arise due to temperature variations, differences in front-end circuitry, and the presence of undesired signals that elevate the noise floor. To model these effects, the elements of the ith row of the matrix $\mathbf{V}\in\mathbb{C}^{m\times n}$, defined in (1), are modeled as zero-mean Gaussian random variables with variance

$$\sigma_i^2=(1+\rho u_i)\bar{\sigma}^2, \tag{3}$$

where u_i is a realization of a uniform random variable U_i over the interval $[-1,1]$, $\bar{\sigma}^2$ is the average noise power at the SUs, and $0\le\rho<1$ is the fraction representing the variability in σ_i^2 around $\bar{\sigma}^2$.

The instantaneous SNR across the SUs, γ, is a random variable due to its dependence on both σ_i^2 and d_i, which are themselves random. Based on (2) and (3), a realization of γ is given by

$$\gamma=\frac{1}{m}\sum_{i=1}^{m}\frac{P_{\mathrm{tx}}\,(d_0/d_i)^{\eta}}{(1+\rho u_i)\bar{\sigma}^2}. \tag{4}$$

Therefore, the average SNR at the SUs is defined as SNR $=\mathbb{E}[\gamma]$, where $\mathbb{E}[\gamma]$ denotes the expected value of γ.

To implement the above SNR model, one first computes the expected value of γ', defined for $\bar{\sigma}^2=1$ and given $\{d_i\}$. It can be shown [11] that this expectation is

$$\mathbb{E}[\gamma']=\ln\left(\frac{1+\rho}{1-\rho}\right)\frac{1}{2\rho m}\sum_{i=1}^{m}P_{\mathrm{rx}i} \tag{5}$$

for $0<\rho<1$, and for $\rho=0$ it becomes

$$\mathbb{E}[\gamma']=\frac{1}{m}\sum_{i=1}^{m}P_{\mathrm{rx}i}. \tag{6}$$

Since SNR $=\mathbb{E}[\gamma]=\mathbb{E}[\gamma']/\bar{\sigma}^2$, the calibrated noise variance is given by

$$\bar{\sigma}^2=\frac{\mathbb{E}[\gamma']}{\mathrm{SNR}}. \tag{7}$$

This value of $\bar{\sigma}^2$ is substituted into (3), along with a realization u_i of the random variable U_i, to obtain σ_i^2, which is the noise variance of the elements in the ith row of $\mathbf{V}$. New values of $\{\sigma_i^2\}$ are generated for each sensing event, thereby introducing the desired temporal variability in noise levels.

The matrix $\mathbf{Y}$ in (1) is constructed at the FC using the mn samples forwarded by the SUs. Under hypothesis $\mathcal{H}_1$, indicating the presence of the PU signal in the sensed band, this matrix is given by $\mathbf{Y}=\mathbf{h}\mathbf{x}^{\mathrm{T}}+\mathbf{V}$. Under hypothesis $\mathcal{H}_0$, indicating the absence of the PU signal, the model reduces to $\mathbf{Y}=\mathbf{V}$. From $\mathbf{Y}$, the FC computes the sample covariance matrix of order $m\times m$, which is given by

$$\mathbf{R}=\frac{1}{n}\mathbf{Y}\mathbf{Y}^{\dagger}, \tag{8}$$

where $\dagger$ denotes the complex conjugate and transpose. The test statistic of the AID is built from the elements of $\mathbf{R}$, as detailed in the next section.

III. The Atkinson index detector

The Atkinson index [14] applied for income inequality measurement is

$$A_\epsilon = 1 - \frac{1}{\bar{r}}\left(\frac{1}{N}\sum_{i=1}^{N} r_i^{1-\epsilon}\right)^{\frac{1}{1-\epsilon}}, \tag{9}$$

where $0 \leq \epsilon \neq 1$ is the inequality aversion parameter, r_i is the income of the ith population or individual, for $i = 1, \ldots, N$, and $\bar{r} = \frac{1}{N}\sum_{i=1}^{N} r_i$ is the mean income.

In [10], the index has been adapted for spectrum sensing, by replacing the incomes r_i by the elements r_{ij} of $\mathbf{R}$, yielding the AID test statistic $T_{\text{AID}} = 1 - A_\epsilon$, which is given by

$$T_{\text{AID}} = \frac{1}{\bar{r}}\left(\sum_{i=1}^{m}\sum_{j=1}^{m} r_{ij}^{1-\epsilon}\right)^{\frac{1}{1-\epsilon}}, \tag{10}$$

where

$$\bar{r} = \frac{1}{m^2}\sum_{i=1}^{m}\sum_{j=1}^{m} r_{ij}. \tag{11}$$

The AID test statistic (10) applies to any value of ϵ, as long as $0 < \epsilon \neq 1$.

When $\epsilon = 0.5$, well-known algorithms for square root calculation can be employed to reduce the computational complexity and latency for calculating T_{AID}, yielding its lowest complexity version

$$T_{\text{AID}} = \frac{1}{\bar{r}}\left(\sum_{i=1}^{m}\sum_{j=i}^{m}(2-I)\sqrt{|r_{ij}| + \Re(r_{ij})}\right)^2, \tag{12}$$

where $I = 1$ for $i = j$ (main diagonal of $\mathbf{R}$), and $I = 0$ for $i \neq j$ (off-diagonal elements).

In [10], the rule for choosing $\epsilon = 0.5$ has been established targeting low time complexity, yet resulting good performance. In the next section, the choice of ϵ is refined by means of the analysis of numerous computer simulation results.

IV. Numerical results

The results presented in this section have been obtained using the MATLAB code [15], from 10000 Monte Carlo simulation runs. Unless otherwise stated, $m = 6$ SUs, SNR $= -10$ dB, path loss exponent $\eta = 2.5$, coverage radius $r = 1$ km, reference distance $d_0 = 1$ m, PU transmit power $P_{\text{tx}} = 5$ W, PU transmitter at $(x, y) = (1, 1)$ km, number of samples $n = 200$, fraction of noise level variation $\rho = 0.5$, mean and standard deviation of the Rice factor $\mu_K = 1.88$ dB and $\sigma_K = 4.13$ dB, and target (constant) probability of false alarm $P_{\text{fa}} = 0.1$.

Fig. 1 shows how the variance of T_{AID} behaves as ϵ is varied from 0.1 to 50. Although not shown, the mean of T_{AID} follows the same pattern. Around $\epsilon = 1$, as expected, both the mean and variance of T_{AID} become extremely unstable, spanning many orders of magnitude, which is consistent with the singularity at $\epsilon = 1$ in (10). At ϵ around 34 and above, missing points (in both mean and variance of T_{AID}) is caused by a NaN values in MATLAB computations, which is owed to a different numerical problem, as explored in the sequel.

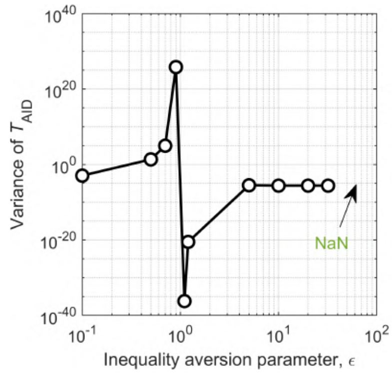

Fig. 1: Variance of T_{AID} versus ϵ.

From the definition of T_{AID}, if $\epsilon = 34$, then $1 - \epsilon = -33$ and $1/(1-\epsilon) = -1/33$. The entries r_{ij} of the sample covariance matrix have magnitudes on the order of 10^{-6} for a typical system setting. Then, raising them to the -33 power leads to extremely large values: $|r_{ij}|^{-33} \approx (10^{-6})^{-33} = 10^{198}$. Such high values, when used in additional calculations, are very likely to exceed the double-precision floating-point range (approximately 10^{308}), causing overflow to Inf during intermediate computations, and, if any operation subsequently involves an undefined form such as Inf − Inf or Inf/Inf, the result becomes NaN.

For example, if the entries of $\mathbf{R}$ satisfy $r_{ij} \sim 10^{-6}$, yielding $|r_{ij}| \in [10^{-8}, 10^{-6}]$, say $|r_{ij}| = 5 \times 10^{-8}$, then $(5 \times 10^{-8})^{-33} \approx 10^{264}$, which may exceed the double-precision representation limits in subsequent calculations. Therefore, intermediate results become Inf, and any subsequent invalid arithmetic with Inf can yield NaN. This confirms that the appearance of NaN values in T_{AID} for large ϵ is a direct consequence of numerical overflow due to raising small values to large negative exponents.

In Fig. 2, the probability of detection of the AID is plotted against the same range of ϵ considered in Fig. 1. It is clear that the useful range of ϵ is in-between 0 and 1, since $P_{\text{d}} \geq P_{\text{fa}}$ in this range. The unitary P_{d} shown by the rightmost point is in fact an invalid outcome that resulted from the previously-described NaN problem.

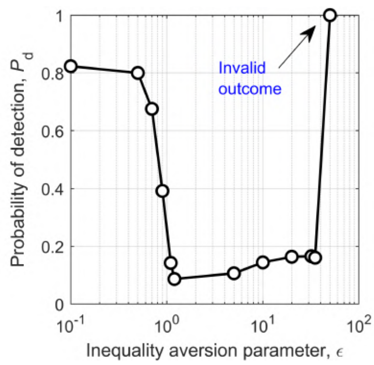

Fig. 2: P_{d} versus ϵ.

Fig. 3 shows P_{d} versus ϵ for ϵ ranging from 0.01 to 0.99, and for different values of the number of SUs, m, while Fig. 4 gives P_d versus m for some values of ϵ. Fig. 3 resembles Fig. 1a of [10], confirming that $\epsilon = 0.5$ is indeed a good choice for acceptable performance and low computational complexity. However, from Fig. 4 it can be realized that $\epsilon = 0.1$ is a better choice if it is expected large numbers of SUs.

The remaining results of this section give further support for the choice of $\epsilon = 0.1$ in the majority of situations, whereas $\epsilon = 0.5$ can be still a good choice in some cases, mainly if low complexity is more relevant than performance.

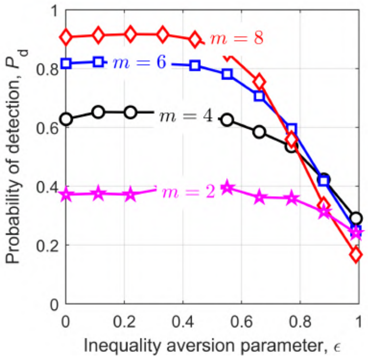

Fig. 3: P_d versus ϵ for different numbers of SUs, m.

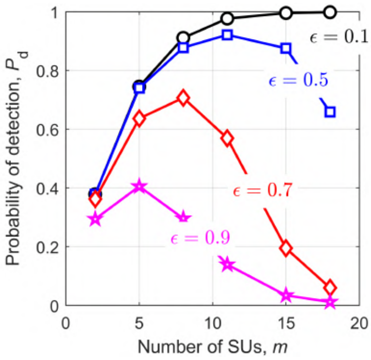

Fig. 4: P_d versus m for different ϵ.

The influences of the number of samples, n, and the SNR on P_d are shown in Fig. 5 and Fig. 6, respectively, for different values of ϵ. In regard to n, $\epsilon = 0.1$ indeed seems to be a good choice, but for moderate-to-small n. If $\epsilon = 0.1$, or even as high as 0.9, good performances are achieved for large values of n. Noteworthy, the performance monotonically improves as n increases, which is an expected outcome.

In regard to the SNR, it can be seen in Fig. 6 that $\epsilon = 0.1$ is also a good choice for the whole SNR range, although larger values of ϵ can be adopted in the unrealistic regimes of very high SNRs. Notice that the performance monotonically improves as the SNR increases, as expected.

Fig. 7 shows the influence of the mean Rice factor on P_d, while Fig. 8 explores how the path loss exponent impacts P_d, both considering some values of ϵ. It can be seen from Fig. 7 that the best choice for ϵ is highly influenced by μ_K. Specifically, $\epsilon = 0.1$ remains a good choice for μ_K above ≈ 2 dB, whereas $\epsilon = 0.5$ or even larger become the most appropriate choice for very small μ_K, which corresponds to a Rayleigh fading channel.

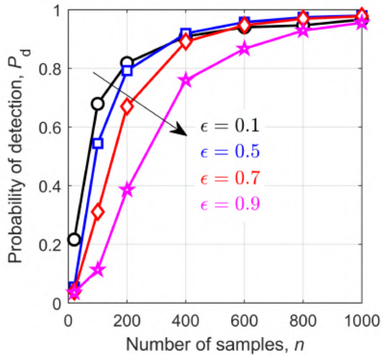

Fig. 5: P_d versus n for different ϵ.

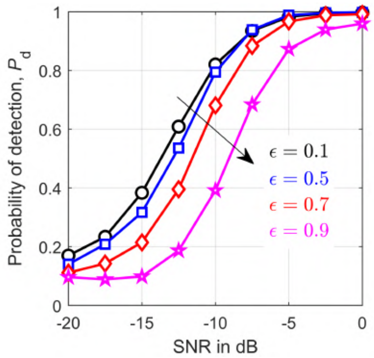

Fig. 6: P_d versus SNR for different ϵ.

As far as η is concerned, Fig. 8 unveils that $\epsilon = 0.1$ remains the best choice for the whole range, with $\epsilon = 0.5$ bringing approximately the same performance.

The performance degradation observed in Fig. 8 as η increases is not credited to a larger average path loss. Instead, it is credited to the larger discrepancies in the signal powers received by the SUs. One must recall that the configured SNR is the same for any η, because the noise power is adjusted accordingly.

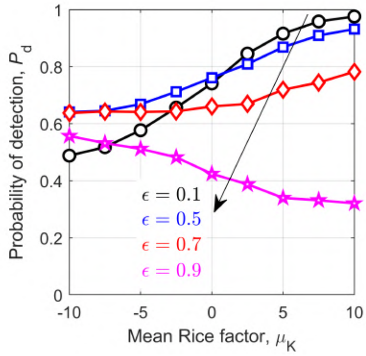

Fig. 7: P_d versus μ_K for different ϵ.

Finally, Fig. 9 and Fig. 10 depict how P_d is influenced by the distances of the PU transmitter to the SUs (as determined by the transmitter coordinates), and by the fraction of noise level variation across the SUs. In both cases, $\epsilon = 0.1$ and $\epsilon = 0.5$ yield comparable performances, with $\epsilon = 0.1$ showing a slight advantage.

The worse performance observed in Fig. 9 for smaller

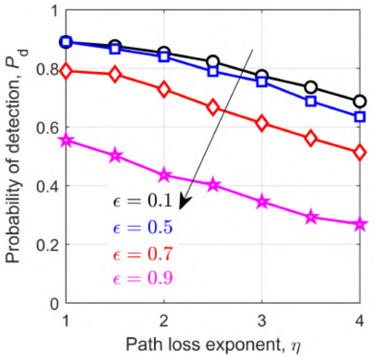

Fig. 8: P_d versus η for different ϵ.

distances from the PU transmitter to the SUs is owed to the larger discrepancies in the received signal powers in comparison with larger distances. Again, one must recall that the configured SNR is the same for any transmitter location, since the noise power is adjusted accordingly.

The small performance variation observed in Fig. 10 highlights the robustness of the AID to noise level variations, which is consistent with the claims presented in [10].

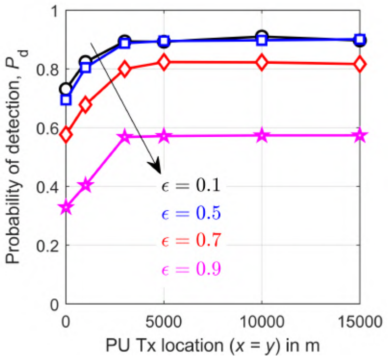

Fig. 9: P_d versus $(x, y = x)$ for different ϵ.

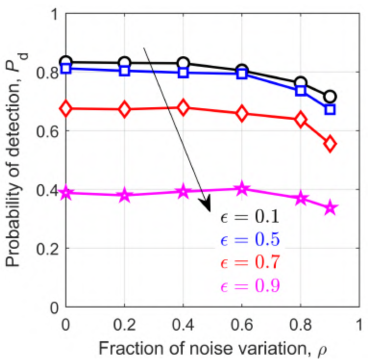

Fig. 10: P_d versus ρ for different ϵ.

V. Conclusions

This paper addressed the influence of the inequality aversion parameter (ϵ) of the Atkinson index detector (AID) on the cooperative spectrum sensing performance. Refining the conclusion drawn in [10], which states that $\epsilon = 0.5$ is a good choice for acceptable performance and low computational complexity, this work examined how ϵ affects the the AID's performance under a variety of circumstances and system parameters.

It has been found that $\epsilon = 0.5$ is indeed the best choice if the aim is a low-complexity computation of the AID test statistic. However, it has been demonstrated that $\epsilon = 0.1$ is the best choice for superior performances in the majority of scenarios of practical significance. It has been also found that $\epsilon = 0.5$ remains a good choice targeting better performance in sensing channels with Rayleigh fading. Numerical problems haven been also highlighted, allowing for the identification of the most useful range of values for ϵ.

References

[1] A. Nasser, H. Al Haj Hassan, J. Abou Chaaya, A. Mansour, and K.-C. Yao, "Spectrum sensing for cognitive radio: Recent advances and future challenge," *Sensors*, vol. 21, no. 7, 2021. [Online]. Available: https://www.mdpi.com/1424-8220/21/7/2408

[2] J. Mitola III and G. Q. Maguire Jr., "Cognitive radio: making software radios more personal," *IEEE Personal Commun. Mag.*, vol. 6, no. 4, pp. 13–18, Aug 1999.

[3] D. A. Guimarães, "Spectrum sensing: A tutorial," *Journal of Communication and Information Systems*, vol. 37, no. 1, pp. 10–29, Feb. 2022. [Online]. Available: https://jcis.sbrt.org.br/jcis/article/view/811

[4] ——, "Gini index inspired robust detector for spectrum sensing over Ricean channels," *Electronics Letters*, November 2018, doi: 10.1049/el.2018.7375.

[5] D. A. Guimarães, "Detector baseado no Índice de Gini e na decomposição de Cholesky para sensoriamento espectral em canais com alto fator de Rice," in *XLI Simpósio Brasileiro de Telecomunicações e Processamento de Sinais, SBrT 2023*, São José dos Campos, SP, Brasil, October 2023.

[6] ——, "Modified Gini index detector for cooperative spectrum sensing over line-of-sight channels," *Sensors*, vol. 23, no. 12, p. 5403, 2023. [Online]. Available: https://www.mdpi.com/1424-8220/23/12/5403

[7] D. A. Guimarães, "Pietra-Ricci index detector for centralized data fusion cooperative spectrum sensing," *IEEE Trans. Veh. Technol.*, vol. 69, no. 10, pp. 12 354–12 358, 2020, doi: 10.1109/TVT.2020.3009440.

[8] D. A. Guimarães, E. J. T. Pereira, and R. Shrestha, "Resource-efficient low-latency modified Pietra-Ricci index detector for spectrum sensing in cognitive radio networks," *IEEE Trans. Veh. Technol.*, pp. 1–15, 2023, doi: 10.1109/TVT.2023.3269345.

[9] D. A. Guimarães, "Detector baseado no Índice de Theil para sensoriamento espectral cooperativo," in *XLII Simpósio Brasileiro de Telecomunicações e Processamento de Sinais, SBrT 2024*, Belém, PA, Brasil, October 2024.

[10] ——, "Atkinson index detector for spectrum sensing," *Journal of Communication and Information Systems, JCIS*, vol. 39, no. 1, pp. 189–193, November 2024, doi: 10.14209/jcis.2024.20.

[11] ——, "Hybrid fusion of Pietra-Ricci index detector information for cooperative spectrum sensing," *Ad Hoc Networks*, vol. 150, p. 103265, 2023. [Online]. Available: https://www.sciencedirect.com/science/article/pii/S1570870523001853

[12] S. Zhu, T. S. Ghazaany, S. M. R. Jones, R. A. Abd-Alhameed, J. M. Noras, T. Van Buren, J. Wilson, T. Suggett, and S. Marker, "Probability distribution of Rician K-factor in urban, suburban and rural areas using real-world captured data," *IEEE Trans. Antennas Propag.*, vol. 62, no. 7, pp. 3835–3839, Jul 2014, doi: 10.1109/TAP.2014.2318072.

[13] T. S. Rappaport, *Wireless Communications: Principles And Practice*, 2nd ed. Pearson Education, 2010.

[14] R. Neves Costa and S. Pérez-Duarte, "Not all inequality measures were created equal - The measurement of wealth inequality, its decompositions, and an application to European household wealth," European Central Bank, Statistics Paper Series, Dec 2019. [Online]. Available: https://www.ecb.europa.eu/pub/pdf/scpsps/ecb.sps31~269c917f9f.en.pdf

[15] D. A. Guimarães, "MATLAB code to simulate the Atkinson index detector (AID) for spectrum sensing," Mar 2025. [Online]. Available: https://www.dropbox.com/scl/fi/b0lxzw6tu1od1ombz6ioc/AID.m?rlkey=4u7nnh744063u8lr4klgyl37g&dl=0